Title

Towards critical and supercritical electromagnetic fields

Authors

Marklund, M

Blackburn, TG

Gonoskov, A

et al.

Publication Date

2023

DOI

10.1017/hpl.2022.46

Peer reviewed

Towards critical and supercritical electromagnetic fields

M. Marklund, T. G. Blackburn, A. Gonoskov, and J. Magnusson
Department of Physics, University of Gothenburg, SE-412 96 Gothenburg, Sweden

S. S. Bulanov
Lawrence Berkeley National Laboratory, Berkeley, California 94720, USA

A. Ilderton
Higgs Centre, School of Physics and Astronomy, University of Edinburgh, EH9 3JZ, UK
(Dated: October 10, 2023)

The availability of ever stronger, laser-generated electromagnetic fields underpins continuing progress in the study and application of nonlinear phenomena in basic physical systems, ranging from molecules and atoms to relativistic plasmas and quantum electrodynamics. This raises the question: how far will we be able to go with future lasers? One exciting prospect is the attainment of field strengths approaching the Schwinger critical field $E_{\rm cr}$ in the laboratory frame, such that the field invariant $E^2 - c^2B^2 > E_{\rm cr}^2$ is reached. The feasibility of doing so has been questioned, on the basis that cascade generation of dense electron-positron plasma would inevitably lead to absorption or screening of the incident light. Here we discuss the potential for future lasers to overcome such obstacles, by combining the concept of multiple colliding laser pulses with that of frequency upshifting via a tailored laser-plasma interaction. This compresses the electromagnetic field energy into a region of nanometer size and attosecond duration, which increases the field magnitude at fixed power but also suppresses pair cascades. Our results indicate that laser facilities with peak power in the tens of PW could be capable of reaching $E_{\rm cr}$. Such a scenario opens up prospects for experimental investigation of phenomena previously considered to occur only in the most extreme environments in the Universe.

I. INTRODUCTION

Progress in high-power laser technology in recent decades has made it possible, through the generation of extraordinarily strong electromagnetic fields, to investigate radiation and particle-production processes in the nonlinear quantum regime [1–10]. In addition, this has opened up new opportunities for the creation of exotic particle and radiation sources [11–21], as well as for studies of electron-positron plasmas [22, 23], which may help to understand various astrophysical processes [24–26].

The nature of laser-matter (or laser-light) interactions is determined by several parameters, including the ratio between the electric field strength E and the Schwinger, or critical, field strength $E_{\rm cr} = m^2c^3/(e\hbar)$ (for c the speed of light, $\hbar$ the reduced Planck constant, m and $e > 0$ the electron mass and charge), see also Appendix A. When $E/E_{\rm cr} \gtrsim 1$ nonlinear quantum effects are expected to be prominent, but the way this is achieved matters. Probing a subcritical field with ultrarelativistic particles, for example, can 'advance' the onset of those quantum effects that depend on the rest-frame ('r.f.') electric field strength via the quantum nonlinearity parameter, $\chi = \gamma E/E_{\rm cr} = E_{\rm r.f.}/E_{\rm cr}$ with $\gamma \gg 1$ being the Lorentz factor. Experimental investigation of such effects is well underway [8, 9, 27, 28]. A different class of physical effects is manifested if we can achieve $E/E_{\rm cr} \gtrsim 1$ in the absence of massive particles, i.e. directly in the lab frame. Such a critical field would be characterised by the invariants $F^2 = (E^2 - c^2B^2)/E_{\rm cr}^2$ and $G^2 = cB.E/E_{\rm cr}^2$ satisfying $F, G \gtrsim 1$. Critical and supercritical ($F, G \gg 1$) fields would modify not only the quantum dynamics of electrons and photons, but also those of heavier particles such as nuclei, and indeed the QED vacuum itself.

However, whether it is even possible to attain the needed high field strengths in the lab frame is an open question [29–34]. This is because such fields would be expected to trigger an electron-positron pair cascade, forming a dense pair plasma that would screen or absorb the laser radiation being focused, preventing the further increase of the field strength [30, 31, 35]. Avoiding the triggering of such a cascade[1] will be essential for maximizing the reachable field strength [32].

In this paper we investigate the possibility to generate supercritical fields by a combination of three essential ideas: advanced focusing, plasma-based conversion of optical or near-IR light to XUV frequencies, and coherent combination of multiple laser pulses (see fig. 1). The conversion to higher frequency has been discussed as a means of reducing the focal volume which increases field strength at fixed power [33, 34, 37–41] (a more detailed discussion can be found

[1] Ultraintense, tightly focused lasers can ponderomotively eject stray particles that might seed a cascade, but this is dependent on the interaction geometry [32, 36].

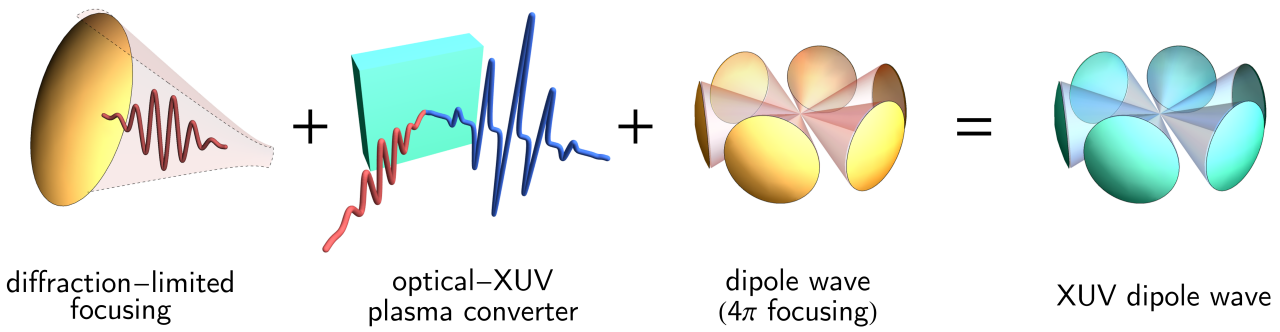

FIG. 1. The main principle behind maximizing field strength starting from laser sources with optical frequencies.

in [42]). Moreover, electromagnetic processes in high strength fields demonstrate a strong dependence on the field wavelength [3]. In combination with 4π focusing, which itself reduces the focal volume, this maximises the electric or magnetic field while suppressing pair cascades, see Appendix B.

Our goal here is to provide a far-future outlook on the field strengths that could be attained in 'best case' scenarios which combine currently known concepts and approaches. We demonstrate numerically that, given advanced focusing, the physics of laser-plasma interactions itself provides the possibility to reach $10E_{\rm cr}$ already out at a laser power of 20 PW. This should certainly be seen as an idealistic (theoretical) reference point, as we omit discussion of a variety of feasibility questions, but it does indicate that further consideration and technological efforts are warranted, with the hope that $E_{\rm cr}$ could be attained at upcoming 10-PW-class laser facilities. This would open up new and exciting opportunities for scientific discoveries, in a regime previously considered to be unattainable. Giving a complete overview of physical applications of strong fields is of course not possible, and we will restrict ourselves here to examples from electron and nuclear physics. This paper is organised as follows. Section II concerns the combination of the three concepts mentioned above: advanced focusing II A, frequency upshifting through plasma-based conversion II B, and coherent combination of multiple laser pulses II C. Section III discusses the impact of such a supercritical field on nuclear and electron dynamics in III A and III B respectively.

II. SETUPS

In this section we provide an order of magnitude estimate for the field strength hypothetically attainable with future laser systems, with the help of the known theoretical ideas outlined above. We start by considering the concepts of 4π focusing and frequency up-shifting separately, before discussing the combination of the two.

A. Advanced focusing

The maximal attainable field strength for a given power of focused radiation is limited by the so-called dipole wave [43] that can also be extended to time-limited solution known as the dipole pulse [44]. The dipole wave can be seen as time-reversed emission of a dipole antenna and thus can be approximated by several focused beams or by focusing intensity-shaped radially-polarized beam with a parabolic mirror [44, 45]. Let us start from considering the benefits of using tight focusing of the laser radiation, characterized by small values of f-number $f_{\rm N}$ or, equivalently, by large values of the divergence angle $\theta = \arctan\left(f_{\rm N}^{-1}/2\right)$, where we for simplicity use the expression that implies $\theta < \pi/2$. To numerically ascertain the potential gain of using tight focusing, we set the initial electromagnetic field to be a two-cycle optical pulse propagating from a spherical surface of radius $r_0 = 16\lambda$, which can be considered large compared to the radiation wavelength λ (the far-field zone):

$$\mathbf{E} = \frac{\mathbf{r}\times[\hat{\mathbf{z}}\times\mathbf{r}]}{|\mathbf{r}\times[\hat{\mathbf{z}}\times\mathbf{r}]|} S_r(r+ct)\, S_\alpha(\alpha)\,, \tag{1}$$

$$\mathbf{B} = \frac{1}{c}\frac{\hat{\mathbf{z}}\times\mathbf{r}}{|\hat{\mathbf{z}}\times\mathbf{r}|} S_r(r+ct)\, S_\alpha(\alpha)\,, \tag{2}$$

where the radial $S_r(r)$ and angular $S_\alpha(\alpha)$ shape functions are defined by:

$$S_r(r) = \sin\left(2\pi(r-r_0)/\lambda\right) \begin{cases} \cos^2\left(\frac{\pi}{2}(r-r_0)/\lambda\right), & |r-r_0| \le \lambda, \\ 0, & |r-r_0| > \lambda, \end{cases} \tag{3}$$

$$S_\alpha(\alpha) = \begin{cases} 1, & \alpha \le \theta - \theta_s/2, \\ \sin^2\left(\frac{\pi}{2}(\alpha-\theta)/\theta_s\right), & \theta - \theta_s/2 < \alpha \le \theta + \theta_s/2, \\ 0, & \alpha > \theta + \theta_s/2, \end{cases} \tag{4}$$

$$\alpha = \arctan\left(\sqrt{z^2+y^2}/|x|\right). \tag{5}$$

In our setup the smoothing angle $\theta_s = 0.3$ eliminates sharp edges of the concave pulse within our model. We advance this field to the vicinity of the focal point using a spectral solver of Maxwells equations within the open-source package hi-χ [46]. To reduce the amount of needed computational resources we also employ the module of contracting a spherical window that maps the concave region of the pulse to a thin layer of space with periodic boundary conditions [47].

The radiation intensity at focus is proportional to the power $\mathcal{P}$ and inversely proportional to the focal spot area, which in turn scales as λ^2 with λ being the radiation wavelength. It is thus possible to express the peak field strength at focus for arbitrary power $\mathcal{P}$ and λ:

$$\frac{E}{E_{\rm cr}} = \frac{\delta}{4.1\times10^5}\left(\frac{\lambda}{1\,\mu{\rm m}}\right)\left(\frac{\mathcal{P}}{1\,{\rm PW}}\right)^{1/2}, \tag{6}$$

where a wavelength-agnostic, dimensionless parameter δ solely characterize the efficiency of focusing. Note that we define it so that $\delta\sqrt{\mathcal{P}/(1\ {\rm PW})}$ gives field amplitude E in relativistic units, i.e. in units of $mc\omega/e$, where ω is radiation frequency. According to our simulations the focusing with f/2 and f/1 provides $\delta \approx 170$ and $\delta \approx 230$, respectively.

A significant improvement can be achieved by splitting the power into 6 pulses and focusing them with $f_{\rm N} = 1$ ($2\theta \approx 0.93 < 2\pi/6$) to the same point symmetrically from different directions in the x-y plane, so that the polarization vector for each pulse is orientated along the z-axis. For each pulse the power is then reduced by a factor of 6 and the field strength reduced by $\sqrt{6}$, but the strength of the combined field multiplies this with a factor of 6 due to coherent summation of the field. As a result we have an increase by factor $\sqrt{6}$: $\delta\,(6\times f/1.0) \approx 560$, which is relatively close to the theoretical maximum $\delta_{\rm max} \approx 780$ provided by the dipole wave [43, 44]. We will use this 6 beam configuration as the main reference for future setups, whereas the configurations with larger number of beams can better sample the dipole wave and bring the value of δ even closer to $\delta_{\rm max}$.

The maximal field strength is achieved either for electric or magnetic field component (pointing along the z-axis), whereas the other field component is close to zero in the center. The maximization of electric field with so-called electric dipole wave provides a strong, oscillating electric field that is especially interesting for enhancing production of electrons and positrons, as well as for trapping them by anomalous radiative trapping [11] that in combination provides unique condition for the creation of radiation sources [14] and extreme plasma states [22, 23]. The maximization of magnetic field by the magnetic dipole wave can also be of interest for initiating extreme plasma dynamics [48] as well as for reaching strong fields with suppressed electromagnetic cascades in the center. The interaction of an *optical* dipole wave with a high energy electron beam leads to the generation of multi-GeV photon sources and can be used as a platform for the study of electromagnetic cascades, of both shower and avalanche type [20, 21]. Finally, a symmetric mixture of electric and magnetic dipole waves provides the optimal setup for attaining highest possible χ value for a given external beam of high-energy electrons [49]. Here we proceed our analysis for electric dipole wave.

B. Plasma converter

The idea and particular concepts for field intensification through plasma-based high-order harmonic generation and focusing have been being discussed by several research groups since the beginning of the 2000s. One possibility is to use the Doppler frequency up-shifting during the reflection of laser radiation from so-called relativistic flying mirrors formed either by the cusp preceding plasma wave breaking [38, 50, 51] or by the ejection of electrons from thin plasma layers [52–56]. In both cases a counter-propagating laser pulse is used to produce the flying mirror that can be shaped to focus the reflected radiation. Another possibility is to use highly-nonlinear reflection of laser radiation from dense plasma naturally formed by ionization of solid targets [57–59]. The early discussions and models also appealed to the Doppler frequency up-shifting, but now during the reflection from oscillating effective boundary [60, 61] that can also be shaped for harmonic focusing by tailoring the pulse intensity shape [39, 62]. It was later recognized that the conversion can be more generally seen as coherent synchrotron emission (CSE) of electrons from a self-generated

Publication, geometry	laser	conversion parameters			yield after focusing		
	peak power, PW	incident intensity, W/cm^2	working plasma density, cm^{-3}	incidence angle	duration, as	intensification factor	peak intensity, W/cm^2
Naumova (2004) [39], plasma denting	–	2×10^{19}	3×10^{21}	0°	200	2.5	5×10^{19}
Gordienko (2005) [40], spherical converter	$\sim5\times10^{-3}$	1.2×10^{19}	5.5×10^{21}	0°	$\lesssim40$	~400	$\sim6\times10^{21}$
Gonoskov (2011) [41], groove-shaped converter	10	5×10^{22}	0.85×10^{23}	62°	~10	4000	2×10^{26}
Baumann (2019) [33], plasma denting	35	1.7×10^{23}	1.7×10^{23}	30°	150	16	2.7×10^{24}
Vincenti (2019) [34], plasma denting	3	10^{22}	–	45°	100	1000	10^{25}

TABLE I. Some of the reported numerical results on focusing plasma-generated XUV pulses.

peripheral layer of electrons [63], while the layer's spring-like dynamics and sought-after emission can be described by a set of differential equations forming so-called relativistic electronic spring (RES) model [41, 64, 65]. Further studies [66] showed that optimal conversion achievable with an incidence angle of $50°-62°$ and the density ramps achievable via tailored pulse contrast [67]. Latest numerical studies exploiting plasma denting in combination with oblique incidence indicate the possibility of significant field intensification [33, 34]. Some of the reported numerical results are summarized in Table I. As a way to estimate future prospects we consider the conversion described in [41, 63].

We performed a number of simulations using a 1D version of the ELMIS PIC code [68] with quantum radiation reaction accounted for via the QED event generator described in [69]. (The oblique incidence is transformed to normal in a moving reference frame [70].) We assumed a single-cycle laser pulse ($\lambda=0.81\,\mu$m) interacting with a steep-front plasma surface with immobile ions. Many factors, including e.g. the motion of ions, plasma spreading due to limited contrast, and pulse shape, can significantly affect both the increase of the amplitude and the optimal conditions for achieving it. However, the physics of this process has been shown to be sufficiently robust to justify the considerations here as a good starting point for further studies [64, 66, 71].

The amplitude increase becomes larger with the increase of incident wave amplitude a_{in}, which we express in relativistic units [72]. We consider two cases $a_{in}\approx70$ ($I=10^{22}\,\mathrm{W/cm^2}$) and $a_{in}\approx220$ ($I=10^{23}\,\mathrm{W/cm^2}$). For each case we fine tune the incidence angle α and the plasma density n expressed in units of plasma critical density. For $I=10^{22}\,\mathrm{W/cm^2}$ we find that the maximal amplitude increase of 8.4 is achieved for $\alpha=61.43°$ and $n=0.4125a_{in}$, whereas for $I=10^{23}\,\mathrm{W/cm^2}$ the maximal amplitude increase of 16.1 is achieved for the same incidence angle but for $n=0.397a_{in}$. For the latter, the resulted field distribution is show in fig. 2(b). The length of the generated pulses in these cases is less than 1 nm, which corresponds to the XUV range.

Although our goal here is to assess the capabilities of the conversion physics itself, we do not consider higher incident intensities, even though these could lead to even higher intensification factors and even shorter pulse duration. One reason for this is that, at higher intensities, QED effects can start to play a detrimental role, due to an increasingly large part of the incident energy being converted into gamma photons (see [73] and Fig. 2 in Ref. [69]). Ion motion is another factor that becomes more prominent with the rise of intensity and makes it difficult to efficiently exploit the conversion mechanism. This motivates further studies on the generation of short pulses [74], exploiting pulse steepening [75–79] and on possibilities to use high-Z, i.e. heavy nuclei, material (note that higher intensity can cause almost complete ionization making charge to mass ratio close to $e/2m_p$ independently of the nuclei type). Finally, for a given incident power, higher intensity at the converter means a smaller area of conversion. Once the characteristic size of the conversion area $r_0/(1\,\mu\mathrm{m})\sim(P/\mathrm{PW})^{1/2}\left[I/(10^{22}\,\mathrm{Wcm^{-2}})\right]^{-1/2}$ becomes comparable to the wavelength $\lambda\sim1\,\mu$m, multidimensional effects start to affect both the conversion process itself, as well as the collimation and synchronization of the XUV pulses generated across the focal area (for two-dimensional numerical studies of the plasma conversion by the considered mechanism see [66, 71]). In this context and for $I=10^{22}\,\mathrm{W/cm^2}$ the minimal power is a few PW, whereas for $I=10^{23}\,\mathrm{W/cm^2}$, it is preferable to have a few tens of PW.

C. Focusing of XUV pulses

We now continue our analysis by considering the possibility of focusing the XUV pulses generated at the curved plasma surfaces of the 6 focusing mirrors with $f_\mathrm{N}=1$. We assume that the laser radiation is split into 6 beams,

pre-focused and delivered so that the optimal conditions for the RES-converters are achieved at the plasma surfaces and the generated XUV pulses become focused at the central point. We assume that the conversion happens at the distance of 6 µm from the centre. We consider two cases: the total power $\mathcal{P}$ is 20 PW and 200 PW, which results in the intensity of 10^{22} W/cm^2 and 10^{23} W/cm^2 at the plasma surfaces, respectively. A rough estimate for the peak field strength achievable in this configuration suggests that for $\mathcal{P} = 20$ PW (200 PW) we can reach $a_{out} \sim 2500$ (8000) given in relativistic units for the wavelength $\lambda \sim 1$ nm, which is well above the Schwinger field strength in both cases. However, this estimate is not sufficient because different spectral fractions are focused to different diffraction-limited volumes. That is why we need to perform numerical calculation to perform estimations for these cases.

In order to resolve the singular XUV peak we use a sequence of adaptive sub-grids that are arranged in the following way. Firstly, we surround the XUV peak with a frame and deduce there the field multiplying by a mask function that smoothly goes from 1 to 0 and the ends of the frame. In such a way we cut out the XUV pulse and the remaining field with narrower spectral content can be sampled with the first grid. We then take the deduced field within the frame and repeat the procedure, introducing another subframe in a closer vicinity of the XUV peak and sampling the remaining field with another more thinner subgrid. We perform this procedure 7 times to reach a sufficient resolution, which in our case corresponds to the space step of 0.064 nm. Every deduced field is advanced first analytically (as a spherical wave) to the distance of 4 frame lengths and then numerically using the spectral solver on the grid 128×512^2.

The result of our numerical calculation for $\mathcal{P} = 200$ PW is shown in fig. 2. The peak field of 130 $E_{\rm cr}$ is achieved in the centre within a volume of about few nanometers in size. The following fit can be used for estimates and calculations:

$$\frac{E(r,t)}{E_{\rm cr}} \approx \mathcal{A}\left(\left|\frac{r+ct}{R}\right|^{3/2}+1\right)^{-1}\left(\left|\frac{ct}{D}\right|+1\right)^{-1}, \tag{7}$$

where $\mathcal{A} = 130$, $R = 0.2$ nm and $D = 0.3$ nm in this case (see the solid black curves in fig. 2 (c)). A similar result is obtained for the case of $\mathcal{P} = 20$ PW, for which we got best fit for $\mathcal{A} = 10$, $R = 0.5$ nm and $D = 0.5$ nm.

The threshold for the cascade can be estimated as the equality of the volume size (distance to the centre) to the mean scale length of pair production. This estimate is shown in fig. 2 (c) with dashed black line and indicates that the region where the field reaches E_s is too small for the occurrence of the cascade based on the Breit-Wheeler process.

We conclude this section by showing schematically the potential of reaching strong fields with different strategies based on a given value of total laser power of a laser facility (see fig. 3). One can see that using tight focusing or, better, multiple colliding laser pulses (MCLP)[80] provides a substantial increase of the peak field, which is, however, well below the Schwinger field even in case of 1 EW total power. The plasma converter can give a significant increase once the intensity of 10^{22} W/cm^2 is reached, which can be provided by $f/1.0$ focusing already with the total laser power of about 100 TW. The conversion at 10^{23} W/cm^2 provides even larger boost. In both cases tight focusing of the generated XUV pulses can provide a significant increase of field strength beyond $E_{\rm cr}$.

Certainly, this analysis is performed under the assumption of best-case scenario and the implementation of such a concept requires many technological advances. Among them, driving plasma conversion and reaching spatial-temporal synchronization of the generated XUV pulses appear to the the central difficulties. However, from our results we can draw a conclusion that achieving the needed spatio-temporal control in the domain of nanometer-attosecond could provide a pathway towards reaching the Schwinger field strength using the outlined concept based on high-intensity laser facilities.

Therefore we estimate that delivering 10 GeV electrons to the strong-field region of the outlined setup would result in a χ of order 10^6, for the case of $P = 20$ PW (see estimates in Appendix B). We will investigate such possibilities in future work.

III. PHYSICAL PROCESSES IN CRITICAL AND SUPERCRITICAL FIELDS

Critical and supercritical fields open up the possibility to perform experiments in regimes that traditionally have not been available to light sources. For the purpose of illustration, we briefly discuss a number of possible studies that could be performed using the extreme-field source we have outlined.

A. Nuclear dynamics

Studies of nuclear photonics have been strongly motivated by using high-brilliance gamma sources for, e.g., excitation of nuclei. However, strong electromagnetic fields can also reach the scales relevant for probing internal nuclear

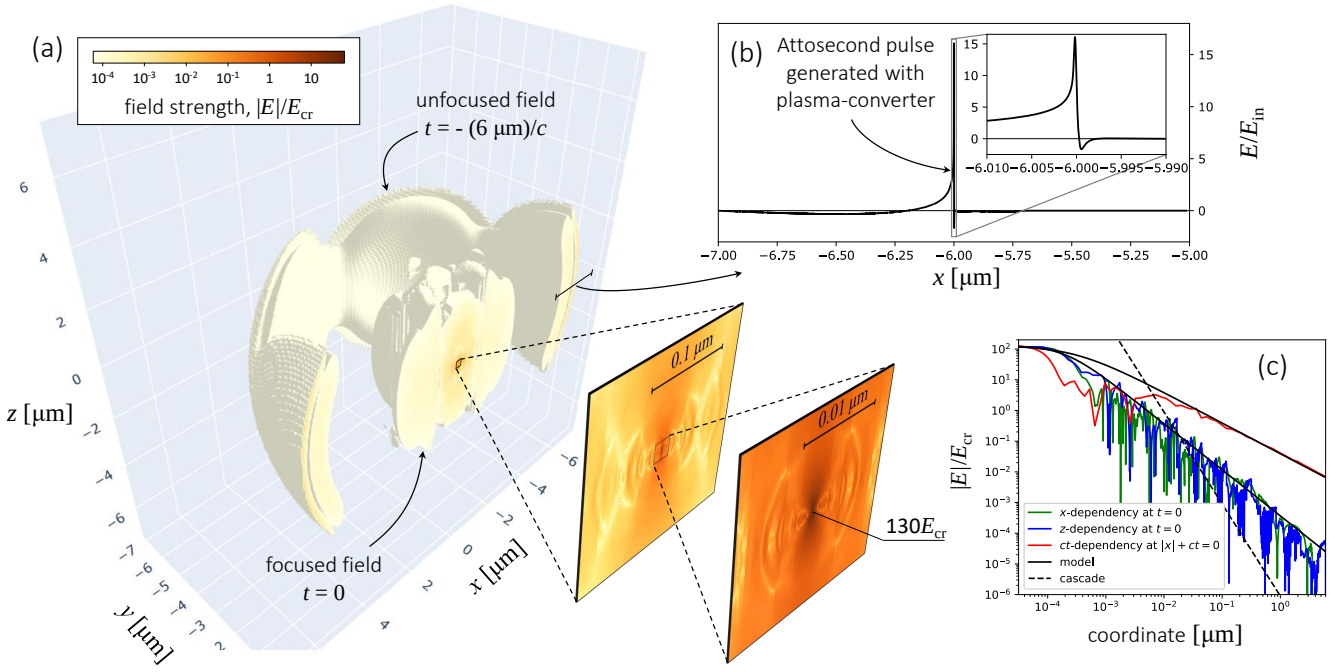

FIG. 2. The numerical result for the dipole focusing of XUV pulses (a). The total laser power of 200 PW is split into 6 beams and each is focused to 10^{23} W/cm^2 at 7 μm from the focus, where the RES-converters provide amplitude boost by factor 15 and frequency upshift by factor $\sim 10^4$ (b). The conversion is followed by the MCLP (e-dipole) focusing using 6 beams at $f/1.0$. The dependency of the field strength on the x-coordinate (green curve), z-coordinate (blue curve) and time (red curve) is shown in panel (c) together with the fit (black solid curves) and the threshold for cascaded pair-generation (dashed black line).

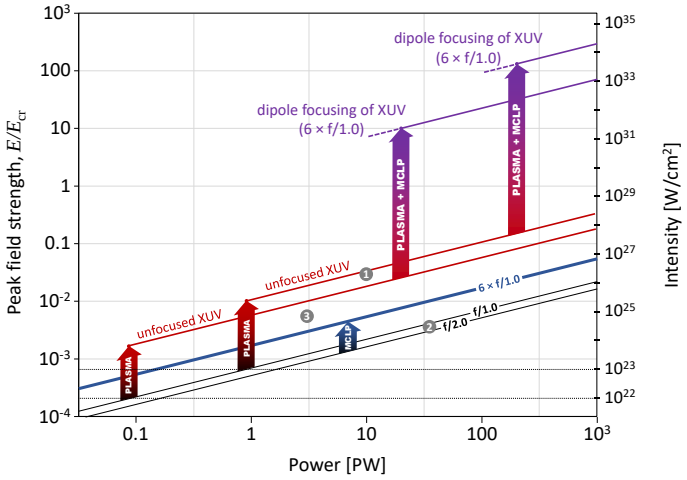

FIG. 3. The prospects of reaching high field strength using tight focusing, multiple laser colliding pulses, the plasma conversion and their combination on the map of the attainable field strength and total power of laser facility. Two outlined options correspond to the use of the plasma conversion at 10^{22} and 10^{23} W/cm^2, respectively. The labels show the results of simulations by Gonoskov et al. [41] (1), by Baumann et al. [33] (2) and by Vincenti [34] (3).

dynamics. Before going further with some examples, we point out that these experiments would give rise to significant challenges, such as the alignment of the target with the focal spot, as well as timing issues. It is still of interest to consider these possibilities, because solid-density plasma can be transparent for the high-intensity XUV pulses. It might also be possible to deliver accelerated nuclei to focus along the dipole pulse axis, where the field strength is greatly suppressed [20]. In this case it might be necessary to accumulate the signal of repeated experiments to compensate for the small size of the strong-field region. To motivate further studies on possible experimental arrangements we discuss some of the possibilities that arise in nuclear physics through the development of strong field

sources.

Electric fields of the strength discussed in section II are sufficient to strip atoms of their electrons; the field strength necessary for barrier-suppression ionization of the deepest lying electron, $E_{\rm BSI} \simeq (Z\alpha)^3 E_{\rm cr}/16$. The bare nucleus can then be accelerated to relativistic velocity, in a single wave period, if the electric-field amplitude $E > E_{\rm rel}$, where

$$\frac{E_{\rm rel}}{E_{\rm cr}} = \frac{A m_p \omega}{eZ} = 3.8\times10^{-3}\,\frac{A}{Z\lambda[\mu{\rm m}]}, \tag{8}$$

and Z and A are the nucleus' atomic and mass numbers. Thus a source of near-critical field could accelerate heavy nuclei from rest to normalised momentum $p/M = 225(Z/A)(E/E_{\rm cr})\lambda[\mu{\rm m}] \gg 1$.

Stronger electric fields affect even the internal dynamics of the nucleus, by modifying the Coulomb barrier through which daughter particles tunnel. For example, the characteristic electric field required to modify the α-decay rate of an unstable nucleus, E_α, can be estimated as [81]

$$\frac{E_\alpha}{E_{\rm cr}} = \frac{2\sqrt{2}Q_\alpha^{5/2}}{3\pi\alpha^2 Z^2 Z_{\rm eff} m_e^2 m_r^{1/2}} \simeq 300\,\frac{Q^{5/2}[{\rm MeV}]}{Z^2 Z_{\rm eff}} \tag{9}$$

where Q is the energy of the α particle, $Z_{\rm eff} = (2A-4Z)/(A+4)$, Z and A are the proton and mass numbers of the daughter nucleus, and m_r is the reduced mass of the α–daughter-nucleus system. For polonium-212, which has a half life of 0.3 ms, $Q \simeq 9.0$ MeV and $E_\alpha/E_{\rm cr} \simeq 30$. The correction to the decay rate $C = \exp[2E(t)\cos\theta/E_\alpha]$, where θ is the angle between the electric-field vector and the α-emission direction. Averaging over all θ, we obtain $\langle C\rangle_\theta = \sinh[2E(t)/E_\alpha]/[2E(t)/E_\alpha]$. Further averaged over a single cycle, with $E(t) = E_0\sin\omega t$, we find that the modification to the decay rate is $\langle C\rangle_{\theta,t} \simeq 1.4$ for $E_0 = 30E_{\rm cr}$ and as much as $\langle C\rangle_{\theta,t} \simeq 21$ for $E_0 = 100E_{\rm cr}$. We note that by exceeding E_α we enter a regime where the effect of the external field is no longer a small correction.

The same logic can be applied to β decay, where the characteristic electric field required to modify the decay rate is [82]:

$$\frac{E_\beta}{E_{\rm cr}} = \left(\frac{2Q_\beta}{m_e}\right)^{3/2} \tag{10}$$

where Q_β is the energy release associated with the decay. In the case of tritium $Q_\beta = 18.6$ keV and $E_\beta = 0.02E_{\rm cr}$. As this is a non-relativistic beta decay, $Q_\beta/m \ll 1$, the modification to the decay rate is $C \simeq (E_0/E_\beta)^{7/3}$, for an applied electric field E_0 which satisfies $E_0/E_\beta \gg 1$ [82]: at $E_0 = 0.1E_{\rm cr}$, $C \simeq 50$.

B. Electron dynamics

A supercritical field structure of this type is a platform for investigating nonlinear quantum electrodynamics in a completely unexplored regime, either by probing it with externally injected electrons or by exploiting the nonlinear dynamics of virtual particles from the quantum vacuum.

Based on an analysis of quantum loop corrections to physical processes in constant, crossed fields, it has been conjectured that the relevant expansion parameter is not the fine structure constant α, small, but rather $\alpha\chi^{2/3}$, which can become large in extremely strong fields [83, 84]. Hence the usual small expansion parameter of perturbative QED becomes, in principle, a large parameter for $\chi > 1600$. In a collision between an electron beam of energy $\mathcal{E}$ and a supercritical electric field of magnitude E, we have that

$$\alpha\chi^{2/3} = 5.3\,\mathcal{E}^{2/3}[10\ {\rm GeV}]\left(\frac{E}{E_{\rm cr}}\right)^{2/3}. \tag{11}$$

Higher-order corrections, normally thought of as *suppressed* by powers of α, are implied by the conjecture to become larger and larger as the order increases. The technical implication is that the perturbative expansion of QED breaks down and needs (somehow) to be resummed [85]; the physical implication is that QED enters a new 'fully nonperturbative' regime in which it behaves as a strongly coupled theory [5, 86]. It is essential that large χ is reached not by simply increasing the particle energy $\mathcal{E}$ at low field strength, as the the Ritus-Narozhny conjecture only applies in the high-intensity (LCFA) regime where $a^3/\chi \gg 1$ [87, 88]. Furthermore, the mitigation of radiative energy losses requires the field duration to be kept as short as possible: for alternative scenarios see [33, 89–92].

Nonlinear quantum dynamics are evident for pure EM fields as well, driven by virtual electron loops that modify the classical linearity of Maxwell's equations. The nonlinear behaviour of a pure magnetic field of strength B, is controlled

by the Heisenberg-Euler interaction Lagrangian (see. e.g., [5, SS7]). At one-loop order, $\mathcal{L} = m^4(B/B_{\rm cr})^4/(360\pi^2)$ for $B \ll B_{\rm cr}$ and $\mathcal{L} = m^4(B/B_{\rm cr})^2\ln(B/B_{\rm cr})/(24\pi^2)$ for $B \gg B_{\rm cr}$. For supercritical magnetic fields, higher-order corrections grow logarithmically, with [93]

$$\frac{\mathcal{L}^{n\text{-loop}}}{\mathcal{L}^{1\text{-loop}}} \sim \left[\frac{\alpha}{\pi}\ln\left(\frac{B}{B_{\rm cr}}\right)\right]^{n-1} . \tag{12}$$

Though this growth is slower than the power-law behaviour of higher-order corrections at ultralarge quantum parameter χ, as predicted (above) in the Ritus-Narozhny conjecture, resummation is still required. Investigating this non-perturbative, non-linear regime of electrodynamics motivates the creation of ultrastrong EM fields that are not probed by ultrarelativistic external particles.

IV. SUMMARY

We have outlined how optimal configurations of laser systems and/or secondary sources could give us the opportunity to approach, or even exceed, the critical field of quantum electrodynamics. The configurations presented certainly constitute immense engineering challenges. Realising an optical-XUV plasma converter demands sophisticated material engineering, high laser contrast and spatial uniformity, as well as timing and pointing stability. The quality of the vacuum is important if observations are to be made of Schwinger pair creation, or of the nuclear physics processes we have considered. These feasibility questions should be addressed in future work. Our results nevertheless indicate that the presented concepts are promising and warrant further analysis. Reaching such critical fields could give an opportunity to probe some of the most extreme environments in the universe, and investigate the behaviour of electrons, nuclei and the quantum vacuum under such conditions. We have given several examples of the use of such new photon sources for probing physical laws, ranging from electron and nuclear physics to probing the quantum vacuum.

ACKNOWLEDGMENTS

The authors would like to thank the anonymous reviewers for their helpful comments. This research was supported by the Swedish Research Council Grants nos. 2016-03329 and 2020-06768 (T.G.B. and M.M.), and 2017-05148 (A.G.), as well as the U.S. Department of Energy Office of Science Offices of High Energy Physics and Fusion Energy Sciences (through LaserNetUS), under Contract No. DE-AC02-05CH11231 (S.S.B.). Simulations were performed on resources provided by the Swedish National Infrastructure for Computing (SNIC).

[1] W. Dittrich and H. Gies, *Probing the quantum vacuum. Perturbative effective action approach in quantum electrodynamics and its application*, Vol. 166 (2000).
[2] A. Di Piazza, C. Muller, K. Z. Hatsagortsyan, and C. H. Keitel, "Extremely high-intensity laser interactions with fundamental quantum systems," Reviews of Modern Physics **84**, 1177–1228 (2012).
[3] P Zhang, S S Bulanov, D Seipt, A V Arefiev, and A. G.R. Thomas, "Relativistic plasma physics in supercritical fields," Physics of Plasmas **27**, 50601 (2020).
[4] A. Gonoskov, T. G. Blackburn, M. Marklund, and S. S. Bulanov, "Charged particle motion and radiation in strong electromagnetic fields," Rev. Mod. Phys. **94**, 045001 (2022).
[5] A. Fedotov, A. Ilderton, F. Karbstein, B. King, D. Seipt, H. Taya, and G. Torgrimsson, "Advances in QED with intense background fields," (2022), arXiv:2203.00019.
[6] C. Bula, K. T. McDonald, E. J. Prebys, C. Bamber, S. Boege, T. Kotseroglou, A. C. Melissinos, D. D. Meyerhofer, W. Ragg, D. L. Burke, R. C. Field, G. Horton-Smith, A. C. Odian, J. E. Spencer, D. Walz, S. C. Berridge, W. M. Bugg, K. Shmakov, and A. W. Weidemann, "Observation of nonlinear effects in compton scattering," Physical Review Letters **76**, 3116–3119 (1996).
[7] D. L. Burke, R. C. Field, G. Horton-Smith, J. E. Spencer, D. Walz, S. C. Berridge, W. M. Bugg, K. Shmakov, A. W. Weidemann, C. Bula, K. T. Mc Donald, E. J. Prebys, C. Bamber, S. J. Boege, T. Koffas, T. Kotseroglou, A. C. Melissinos, D. D. Meyerhofer, D. A. Reis, and W. Ragg, "Positron production in multiphoton light-by-light scattering," Physical Review Letters **79**, 1626–1629 (1997).
[8] J. M. Cole, K. T. Behm, E. Gerstmayr, T. G. Blackburn, J. C. Wood, C. D. Baird, M. J. Duff, C. Harvey, A. Ilderton, A. S. Joglekar, K. Krushelnick, S. Kuschel, M. Marklund, P. McKenna, C. D. Murphy, K. Poder, C. P. Ridgers, G. M. Samarin, G. Sarri, D. R. Symes, A. G. R. Thomas, J. Warwick, M. Zepf, Z. Najmudin, and S. P. D. Mangles, "Experimental evidence of radiation reaction in the collision of a high-intensity laser pulse with a laser-wakefield accelerated electron beam," Physical Review X **8**, 011020 (2018).

[9] K Poder, M Tamburini, G Sarri, A Di Piazza, S Kuschel, C D Baird, K Behm, S Bohlen, J M Cole, D J Corvan, M Duff, E Gerstmayr, C H Keitel, K Krushelnick, S. P.D. Mangles, P McKenna, C D Murphy, Z Najmudin, C P Ridgers, G M Samarin, D R Symes, A. G.R. Thomas, J Warwick, and M Zepf, "Experimental Signatures of the Quantum Nature of Radiation Reaction in the Field of an Ultraintense Laser," Physical Review X **8**, 31004 (2018).

[10] Jin Woo Yoon, Yeong Gyu Kim, Il Choi, Jae Hee Sung, H. W. Lee, Seong Ku Lee, and Chang Hee Nam, "Realization of laser intensity over 10 W/cm," Optica **8**, 630–635 (2021).

[11] A. Gonoskov, A. Bashinov, I. Gonoskov, C. Harvey, A. Ilderton, A. Kim, M. Marklund, G. Mourou, and A. Sergeev, "Anomalous radiative trapping in laser fields of extreme intensity," Phys. Rev. Lett. **113**, 014801 (2014).

[12] D. J. Stark, T. Toncian, and A. V. Arefiev, "Enhanced multi-mev photon emission by a laser-driven electron beam in a self-generated magnetic field," Phys. Rev. Lett. **116**, 185003 (2016).

[13] Matteo Tamburini, Antonino Di Piazza, and Christoph H Keitel, "Laser-pulse-shape control of seeded QED cascades," Scientific Reports **7**, 5694 (2017).

[14] A. Gonoskov, A. Bashinov, S. Bastrakov, E. Efimenko, A. Ilderton, A. Kim, M. Marklund, I. Meyerov, A. Muraviev, and A. Sergeev, "Ultrabright gev photon source via controlled electromagnetic cascades in laser-dipole waves," Phys. Rev. X **7**, 041003 (2017).

[15] Erik Wallin, Arkady Gonoskov, and Mattias Marklund, "Radiation emission from braided electrons in interacting wake-fields," Physics of Plasmas **24**, 093101 (2017).

[16] Bifeng Lei, Jingwei Wang, Vasily Kharin, Matt Zepf, and Sergey Rykovanov, "γ-ray generation from plasma wakefield resonant wiggler," Phys. Rev. Lett. **120**, 134801 (2018).

[17] Marija Vranic, Ondrej Klimo, Georg Korn, and Stefan Weber, "Multi-GeV electron-positron beam generation from laser-electron scattering," Scientific Reports **8**, 4702 (2018).

[18] Alberto Benedetti, Matteo Tamburini, and Christoph H. Keitel, "Giant collimated gamma-ray flashes," Nature Photonics **12**, 319–323 (2018).

[19] O Jansen, T Wang, D J Stark, E d'Humières, T Toncian, and A V Arefiev, "Leveraging extreme laser-driven magnetic fields for gamma-ray generation and pair production," Plasma Physics and Controlled Fusion **60**, 054006 (2018).

[20] J. Magnusson, A. Gonoskov, M. Marklund, T. Zh. Esirkepov, J. K. Koga, K. Kondo, M. Kando, S. V. Bulanov, G. Korn, and S. S. Bulanov, "Laser-particle collider for multi-gev photon production," Phys. Rev. Lett. **122**, 254801 (2019).

[21] J. Magnusson, A. Gonoskov, M. Marklund, T. Zh. Esirkepov, J. K. Koga, K. Kondo, M. Kando, S. V. Bulanov, G. Korn, C. G. R. Geddes, C. B. Schroeder, E. Esarey, and S. S. Bulanov, "Multiple colliding laser pulses as a basis for studying high-field high-energy physics," Phys. Rev. A **100**, 063404 (2019).

[22] Evgeny S Efimenko, Aleksei V Bashinov, Sergei I Bastrakov, Arkady A Gonoskov, Alexander A Muraviev, Iosif B Meyerov, Arkady V Kim, and Alexander M Sergeev, "Extreme plasma states in laser-governed vacuum breakdown," Scientific Reports **8**, 2329 (2018).

[23] E. S. Efimenko, A. V. Bashinov, A. A. Gonoskov, S. I. Bastrakov, A. A. Muraviev, I. B. Meyerov, A. V. Kim, and A. M. Sergeev, "Laser-driven plasma pinching in e-e+ cascade," Physical Review E **99**, 031201 (2019).

[24] Roberto Turolla, Silvia Zane, and Anna Watts, "Magnetars: the physics behind observations. A review," Rept. Prog. Phys. **78**, 116901 (2015), arXiv:1507.02924 [astro-ph.HE].

[25] Victoria M. Kaspi and Andrei Beloborodov, "Magnetars," Ann. Rev. Astron. Astrophys. **55**, 261–301 (2017), arXiv:1703.00068 [astro-ph.HE].

[26] Chul Min Kim and Sang Pyo Kim, "Magnetars as Laboratories for Strong Field QED," in *17th Italian-Korean Symposium on Relativistic Astrophysics* (2021) arXiv:2112.02460 [astro-ph.HE].

[27] Halina Abramowicz *et al.* (LUXE collaboration), "Conceptual Design Report for the LUXE Experiment," European Physical Journal: Special Topics **230**, 2445–2560 (2021).

[28] V Yakimenko, L Alsberg, E Bong, G Bouchard, C Clarke, C Emma, S Green, C Hast, M J Hogan, J Seabury, N Lipkowitz, B O'Shea, D Storey, G White, and G Yocky, "FACET-II facility for advanced accelerator experimental tests," Physical Review Accelerators and Beams **22**, 101301 (2019).

[29] S S Bulanov, N B Narozhny, V D Mur, and V S Popov, "Electron-positron pair production by electromagnetic pulses," Journal of Experimental and Theoretical Physics **102**, 9–23 (2006).

[30] A. M. Fedotov, N. B. Narozhny, G. Mourou, and G. Korn, "Limitations on the attainable intensity of high power lasers," Physical Review Letters **105**, 080402 (2010).

[31] Stepan S. Bulanov, Timur Zh. Esirkepov, Alexander G.R. Thomas, James K Koga, and Sergei V Bulanov, "Schwinger limit attainability with extreme power lasers," Physical Review Letters **105**, 220407 (2010).

[32] A. Gonoskov, I. Gonoskov, C. Harvey, A. Ilderton, A. Kim, M. Marklund, G. Mourou, and A. Sergeev, "Probing nonperturbative QED with optimally focused laser pulses," Phys. Rev. Lett. **111**, 060404 (2013).

[33] C. Baumann, E. N. Nerush, A. Pukhov, and I. Yu Kostyukov, "Probing non-perturbative QED with electron-laser collisions," Scientific Reports **9**, 1–8 (2019).

[34] Henri Vincenti, "Achieving extreme light intensities using optically curved relativistic plasma mirrors," Phys. Rev. Lett. **123**, 105001 (2019).

[35] E. N. Nerush, I. Yu. Kostyukov, A. M. Fedotov, N. B. Narozhny, N. V. Elkina, and H. Ruhl, "Laser field absorption in self-generated electron-positron pair plasma," Physical Review Letters **106**, 035001 (2011).

[36] A. Sampath and M. Tamburini, "Towards realistic simulations of QED cascades: Non-ideal laser and electron seeding effects," Phys. Plasmas **25**, 083104 (2018).

[37] K. Landecker, "Possibility of frequency multiplication and wave amplification by means of some relativistic effects," Phys. Rev. **86**, 852–855 (1952).

[38] Sergei V. Bulanov, Timur Esirkepov, and Toshiki Tajima, "Light Intensification towards the Schwinger Limit," Phys. Rev. Lett. **91**, 085001 (2003).

[39] N. M. Naumova, J. A. Nees, I. V. Sokolov, B. Hou, and G. A. Mourou, "Relativistic generation of isolated attosecond pulses in a λ^3 focal volume," Phys. Rev. Lett. **92**, 063902 (2004).

[40] S. Gordienko, A. Pukhov, O. Shorokhov, and T. Baeva, "Coherent focusing of high harmonics: A new way towards the extreme intensities," Phys. Rev. Lett. **94**, 103903 (2005).

[41] A. A. Gonoskov, A. V. Korzhimanov, A. V. Kim, M. Marklund, and A. M. Sergeev, "Ultrarelativistic nanoplasmonics as a route towards extreme-intensity attosecond pulses," Phys. Rev. E **84**, 046403 (2011).

[42] Sergei V Bulanov, Timur Zh. Esirkepov, Masaki Kando, Aleksandr S Pirozhkov, and Nikolai N Rosanov, "Relativistic mirrors in plasmas novel results and perspectives," Uspekhi Fizicheskih Nauk **183**, 449–486 (2013).

[43] I M Bassett, "Limit to Concentration by Focusing," Opt. Acta **33**, 279–286 (1986).

[44] Ivan Gonoskov, Andrea Aiello, Simon Heugel, and Gerd Leuchs, "Dipole pulse theory: Maximizing the field amplitude from 4π focused laser pulses," Phys. Rev. A **86**, 053836 (2012).

[45] Tae Moon Jeong, Sergei Vladimirovich Bulanov, Pavel Vasilievich Sasorov, Stepan Sergeevich Bulanov, James Kevin Koga, and Georg Korn, "4π-spherically focused electromagnetic wave: diffraction optics approach and high-power limits," Optics Express **28**, 13991 (2020).

[46] The Hi-Chi Project, "Hi-chi," (2022).

[47] Elena Panova, Valentin Volokitin, Evgeny Efimenko, Julien Ferri, Thomas Blackburn, Mattias Marklund, Alexander Muschet, Aitor De Andres Gonzalez, Peter Fischer, Laszlo Veisz, Iosif Meyerov, and Arkady Gonoskov, "Optimized computation of tight focusing of short pulses using mapping to periodic space," Applied Sciences **11**, 956 (2021).

[48] A. V. Bashinov, E. S. Efimenko, A. A. Muraviev, V. D. Volokitin, I. B. Meyerov, G. Leuchs, A. M. Sergeev, and A. V. Kim, "Particle trajectories, gamma-ray emission, and anomalous radiative trapping effects in magnetic dipole wave," Phys. Rev. E **105**, 065202 (2022).

[49] Christoffer Olofsson and Arkady Gonoskov, "Bi-dipole wave: optimum for attaining extreme regimes at matter-light colliders," (2022), arXiv:2202.08251.

[50] S F Martins, J P Santos, R A Fonseca, and L O Silva, "Pulse Compression and Frequency Up-Shift with Nonlinear Plasma Waves," Physica Scripta **2004**, 118 (2004).

[51] N. H. Matlis, S. Reed, S. S. Bulanov, V. Chvykov, G. Kalintchenko, T. Matsuoka, P. Rousseau, V. Yanovsky, A. Maksimchuk, S. Kalmykov, G. Shvets, and M. C. Downer, "Snapshots of laser wakefields," Nature Physics **2**, 749–753 (2006).

[52] Victor V. Kulagin, Vladimir A. Cherepenin, Min Sup Hur, and Hyyong Suk, "Theoretical Investigation of Controlled Generation of a Dense Attosecond Relativistic Electron Bunch from the Interaction of an Ultrashort Laser Pulse with a Nanofilm," Physical Review Letters **99**, 124801 (2007).

[53] J. Meyer-Ter-Vehn and H. C. Wu, "Coherent Thomson backscattering from laser-driven relativistic ultra-thin electron layers," European Physical Journal D **55**, 433–441 (2009).

[54] D. Habs, M. Hegelich, J. Schreiber, M. Gross, A. Henig, D. Kiefer, and D. Jung, "Dense laser-driven electron sheets as relativistic mirrors for coherent production of brilliant X-ray and γ-ray beams," Applied Physics B: Lasers and Optics **93**, 349–354 (2008).

[55] S. S. Bulanov, A. Maksimchuk, K. Krushelnick, K. I. Popov, V. Yu Bychenkov, and W. Rozmus, "Ensemble of ultra-high intensity attosecond pulses from laser-plasma interaction," Physics Letters, Section A: General, Atomic and Solid State Physics **374**, 476–480 (2010).

[56] T. Zh Esirkepov, S. V. Bulanov, M. Kando, A. S. Pirozhkov, and A. G. Zhidkov, "Boosted high-harmonics pulse from a double-sided relativistic mirror," Physical Review Letters **103**, 025002 (2009).

[57] S. V. Bulanov, N. M. Naumova, and F. Pegoraro, "Interaction of an ultrashort, relativistically strong laser pulse with an overdense plasma," Physics of Plasmas **1**, 745–757 (1994).

[58] R Lichters, J Meyer-ter Vehn, and A Pukhov, "Shortpulse laser harmonics from oscillating plasma surfaces driven at relativistic intensity," Phys. Plasmas **3**, 3425–3437 (1996).

[59] D von der Linde and K Rzàzewski, "High-order optical harmonic generation from solid surfaces," Appl. Phys. B **63**, 499–506 (1996).

[60] S. Gordienko, A. Pukhov, O. Shorokhov, and T. Baeva, "Relativistic doppler effect: Universal spectra and zeptosecond pulses," Phys. Rev. Lett. **93**, 115002 (2004).

[61] T. Baeva, S. Gordienko, and A. Pukhov, "Theory of high-order harmonic generation in relativistic laser interaction with overdense plasma," Phys. Rev. E **74**, 046404 (2006).

[62] B. Dromey, D. Adams, R. Hörlein, Y. Nomura, S. G. Rykovanov, D. C. Carroll, P. S. Foster, S. Kar, K. Markey, P. McKenna, D. Neely, M. Geissler, G. D. Tsakiris, and M. Zepf, "Diffraction-limited performance and focusing of high harmonics from relativistic plasmas," Nature Physics **5**, 146–152 (2009).

[63] D. An Der Brügge and A. Pukhov, "Enhanced relativistic harmonics by electron nanobunching," Physics of Plasmas **17**, 033110 (2010).

[64] Arkady Gonoskov, "Theory of relativistic radiation reflection from plasmas," Physics of Plasmas **25**, 013108 (2018).

[65] M Blanco, M T Flores-Arias, and A Gonoskov, "Controlling the ellipticity of attosecond pulses produced by laser irradiation of overdense plasmas," Phys. Plasmas **25**, 093114 (2018).

[66] T. G. Blackburn, A. A. Gonoskov, and M. Marklund, "Relativistically intense XUV radiation from laser-illuminated near-critical plasmas," Physical Review A **98**, 023421 (2018).

[67] C. Rödel, D. an der Brügge, J. Bierbach, M. Yeung, T. Hahn, B. Dromey, S. Herzer, S. Fuchs, A. Galestian Pour, E. Eckner, M. Behmke, M. Cerchez, O. Jäckel, D. Hemmers, T. Toncian, M. C. Kaluza, A. Belyanin, G. Pretzler, O. Willi, A. Pukhov,

M. Zepf, and G. G. Paulus, "Harmonic generation from relativistic plasma surfaces in ultrasteep plasma density gradients," Phys. Rev. Lett. **109**, 125002 (2012).
[68] Arkady Gonoskov, *Ultra-intense laser-plasma interaction for applied and fundamental physics*, Ph.D. thesis, Umea universitet (2013).
[69] A Gonoskov, S Bastrakov, E Efimenko, A Ilderton, M Marklund, I Meyerov, A Muraviev, A Sergeev, I Surmin, and E Wallin, "Extended particle-in-cell schemes for physics in ultrastrong laser fields: Review and developments," Physical Review E **92**, 023305 (2015).
[70] A. Bourdier, "Oblique incidence of a strong electromagnetic wave on a cold inhomogeneous electron plasma. relativistic effects," Physics of Fluids **26**, 1804 (1983).
[71] Shikha Bhadoria, Thomas Blackburn, Arkady Gonoskov, and Mattias Marklund, "Mapping the power-law decay of high-harmonic spectra from few-cycle laser–solid interactions," Phys. Plasmas **29**, 093109 (2022).
[72] A.V. Bashinov, A.A. Gonoskov, A.V. Kim, G. Mourou, and A.M. Sergeev, "New horizons for extreme light physics with mega-science project XCELS," The European Physical Journal Special Topics **223**, 1105–1112 (2014).
[73] E. N. Nerush, I. Yu. Kostyukov, L. Ji, and A. Pukhov, "Gamma-ray generation in ultrahigh-intensity laser-foil interactions," Physics of Plasmas **21**, 013109 (2014).
[74] D. E. Rivas, A. Borot, D. E. Cardenas, G. Marcus, X. Gu, D. Herrmann, J. Xu, J. Tan, D. Kormin, G. Ma, W. Dallari, G. D. Tsakiris, I. B. Földes, S. w. Chou, M. Weidman, B. Bergues, T. Wittmann, H. Schröder, P. Tzallas, D. Charalambidis, O. Razskazovskaya, V. Pervak, F. Krausz, and L. Veisz, "Next generation driver for attosecond and laser-plasma physics," Scientific Reports **7** (2017), 10.1038/s41598-017-05082-w.
[75] T. K. Gustafson, J. P. Taran, H. A. Haus, J. R. Lifsitz, and P. L. Kelley, "Self-modulation, self-steepening, and spectral development of light in small-scale trapped filaments," Physical Review **177**, 306–313 (1969).
[76] Predhiman Kaw, "Relativistic nonlinear propagation of laser beams in cold overdense plasmas," Physics of Fluids **13**, 472 (1970).
[77] A. A. Gonoskov, A. V. Korzhimanov, V. I. Eremin, A. V. Kim, and A. M. Sergeev, "Multicascade proton acceleration by a superintense laser pulse in the regime of relativistically induced slab transparency," Physical Review Letters **102** (2009), 10.1103/physrevlett.102.184801.
[78] Stephen A. Reed, Takeshi Matsuoka, Stepan Bulanov, Motonobu Tampo, Vladimir Chvykov, Galina Kalintchenko, Pascal Rousseau, Victor Yanovsky, Ryousuke Kodama, Dale W. Litzenberg, Karl Krushelnick, and Anatoly Maksimchuk, "Relativistic plasma shutter for ultraintense laser pulses," Applied Physics Letters **94**, 201117 (2009).
[79] H. Y. Wang, C. Lin, Z. M. Sheng, B. Liu, S. Zhao, Z. Y. Guo, Y. R. Lu, X. T. He, J. E. Chen, and X. Q. Yan, "Laser shaping of a relativistic intense, short gaussian pulse by a plasma lens," Physical Review Letters **107** (2011), 10.1103/physrevlett.107.265002.
[80] S. S. Bulanov, V. D. Mur, N. B. Narozhny, J. Nees, and V. S. Popov, "Multiple colliding electromagnetic pulses: A way to lower the threshold of e^+e^- pair production from vacuum," Phys. Rev. Lett. **104**, 220404 (2010).
[81] Adriana Pálffy and Sergey V. Popruzhenko, "Can extreme electromagnetic fields accelerate the α decay of nuclei?" Phys. Rev. Lett. **124**, 212505 (2020).
[82] E. Kh. Akhmedov, "Beta decay and other processes in strong electromagnetic fields," Physics of Atomic Nuclei **74**, 12991315 (2011).
[83] V I Ritus, "Radiative effects and their enhancement in an intense electromagnetic field," Sov. Phys. JETP **30**, 1181 (1970).
[84] N. B. Narozhny, "Expansion parameter of perturbation theory in intense-field quantum electrodynamics," Physical Review D **21**, 1176–1183 (1980).
[85] T. Heinzl, A. Ilderton, and B. King, "Classical Resummation and Breakdown of Strong-Field QED," Phys. Rev. Lett. **127**, 061601 (2021), arXiv:2101.12111 [hep-ph].
[86] A. M. Fedotov, "Conjecture of perturbative QED breakdown at $\alpha\chi^{2/3} \gtrsim 1$," J. Phys. Conf. Ser. **826**, 012027 (2017), arXiv:1608.02261 [hep-ph].
[87] T. Podszus and A. Di Piazza, "High-energy behavior of strong-field QED in an intense plane wave," Phys. Rev. D **99**, 076004 (2019), arXiv:1812.08673 [hep-ph].
[88] A. Ilderton, "Note on the conjectured breakdown of QED perturbation theory in strong fields," Phys. Rev. D **99**, 085002 (2019), arXiv:1901.00317 [hep-ph].
[89] T. G. Blackburn, A. Ilderton, M. Marklund, and C. P. Ridgers, "Reaching supercritical field strengths with intense lasers," New Journal of Physics **21**, 053040 (2019).
[90] V. Yakimenko, S. Meuren, F. Del Gaudio, C. Baumann, A. Fedotov, F. Fiuza, T. Grismayer, M. J. Hogan, A. Pukhov, L. O. Silva, and G. White, "Prospect of Studying Nonperturbative QED with Beam-Beam Collisions," Physical Review Letters **122**, 190404 (2019).
[91] A. Di Piazza, T. N. Wistisen, M. Tamburini, and U. I. Uggerhøj, "Testing strong field qed close to the fully nonperturbative regime using aligned crystals," Phys. Rev. Lett. **124**, 044801 (2020).
[92] Matteo Tamburini and Sebastian Meuren, "Efficient high-energy photon production in the supercritical qed regime," Phys. Rev. D **104**, L091903 (2021).
[93] Felix Karbstein, "All-loop result for the strong magnetic field limit of the Heisenberg-Euler effective Lagrangian," Phys. Rev. Lett. **122**, 211602 (2019).

Appendix A: Invariants

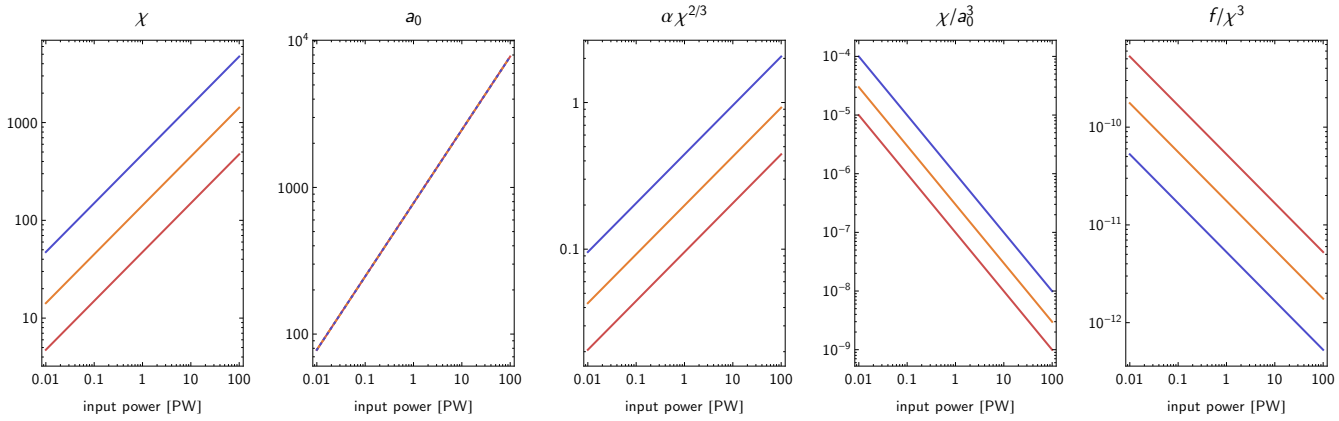

FIG. 4. The invariants that characterize the interaction between an ultrarelativistic electron ($\gamma_0 = 2\times10^4$) and a dipole wave generated by 4π-focusing of a given input power at $\lambda = 0.8\,\mu$m (red) and the third and tenth harmonics (orange, purple).

Consider the interaction of an electron with Lorentz factor γ_0 and a dipole wave that has maximum normalized field strength $\varepsilon \equiv E_0/E_{\rm cr}$ and frequency ω. The three most important invariants are: the quantum nonlinearity parameter $\chi = \gamma_0\varepsilon$; the classical nonlinearity parameter $a_0 = \varepsilon m/\omega$; and the field strength $f = \varepsilon^2$. In terms of the electron energy $\mathcal{E}_0$, the input power $\mathcal{P}$ and wavelength $\lambda = 2\pi/\omega$, these are:

$$\chi = 3.7\frac{\mathcal{E}_0\,[\mathrm{GeV}]\mathcal{P}^{1/2}\,[\mathrm{PW}]}{\lambda\,[\mu\mathrm{m}]}, \qquad a_0 = 780\mathcal{P}^{1/2}\,[\mathrm{PW}], \qquad f = 3.6\times10^{-6}\frac{\mathcal{P}\,[\mathrm{PW}]}{\lambda^2\,[\mu\mathrm{m}]}. \tag{A1}$$

Besides these three, we have the following:

$$\alpha\chi^{2/3} = 0.017\frac{\mathcal{E}_0^{2/3}\,[\mathrm{GeV}]\mathcal{P}^{1/3}\,[\mathrm{PW}]}{\lambda^{2/3}\,[\mu\mathrm{m}]}, \quad \frac{\chi}{a_0^3} = 7.8\times10^{-9}\frac{\mathcal{E}_0\,[\mathrm{GeV}]}{\mathcal{P}\,[\mathrm{PW}]\lambda\,[\mu\mathrm{m}]}, \quad \frac{f}{\chi^3} = 7.0\times10^{-8}\frac{\lambda\,[\mu\mathrm{m}]}{\mathcal{E}_0^3\,[\mathrm{GeV}]\mathcal{P}^{1/2}\,[\mathrm{PW}]}. \tag{A2}$$

These determine the importance of radiative corrections, non-local effects, and background-field-driven processes (e.g. Schwinger pair creation [32]), respectively. They are plotted along with χ and a_0 in fig. 4 for an electron with $\gamma_0 = 2\times10^4$. The locally constant, crossed field approximation (LCFA), a standard assumption in simulation codes, requires both $\chi/a_0^3 \ll 1$ and $f/\chi^3 \ll 1$.

Appendix B: Pair cascades

For sufficiently strong laser fields it becomes possible to generate electron-positron pairs through the Schwinger mechanism. Even in a perfect vacuum, this opens up the possibility for the creation of seed particles that can in turn trigger an avalanche-type pair production cascade through the non-linear Breit-Wheeler process. However, since these two processes work over different time and length scales, it may be possible to produce a large number of electron-positron pairs through the Schwinger mechanism, without necessarily triggering an avalanche cascade.

The number of electron-positron pairs that can be produced through the Schwinger mechanism is given by

$$N_p^{\rm Schwinger} = \frac{1}{4\pi^3\lambda_{\rm C}^4}\int dx^4\mathscr{E}^2\exp(-\pi/\mathscr{E}), \tag{B1}$$

where $\mathscr{E} = \sqrt{|\mathcal{S}| + \mathcal{S}}/E_{\rm cr}$, with $\mathcal{S} = \frac{1}{2}(\mathbf{E}^2 - c^2\mathbf{B}^2)$ and assuming that $\mathbf{E}\cdot c\mathbf{B} = 0$. Here it is also assumed that the characteristic scale of Schwinger pair production is much smaller than the characteristic scale of the electromagnetic field, such that the total number of pairs can be obtained by integrating the local pair production rate over the 4-volume [29].

As can be seen in equation B1, the pair production is strongly dependent on the field strength. In Table II we present the estimated peak field values of four different field configurations: (1) an $f/1$-focused optical field; (2) a

$\mathcal{P}$, PW	$f/1$-focusing		4π-focusing		Frequency upshifting + $f/1$-focusing		Frequency upshifting + $6\times f/1$-focusing	
	$E_0/E_{\rm cr}$	χ_0	$E_0/E_{\rm cr}$	χ_0	$E_0/E_{\rm cr}$	χ_0	$E_0/E_{\rm cr}$	χ_0
1	6.9×10^{-4}	13.6	2.3×10^{-3}	46.0	0.913	$\mathbf{1.8\times10^{4}}$	2.2	$\mathbf{4.4\times10^{4}}$
10	2.2×10^{-3}	42.9	7.4×10^{-3}	145	2.89	$\mathbf{5.6\times10^{4}}$	7.1	$\mathbf{1.4\times10^{5}}$
100	6.9×10^{-3}	136	2.3×10^{-2}	460	9.13	$\mathbf{1.8\times10^{5}}$	22	$\mathbf{4.4\times10^{5}}$
1000	2.2×10^{-2}	429	7.4×10^{-2}	1450	28.9	$\mathbf{5.6\times10^{5}}$	71	$\mathbf{1.4\times10^{6}}$

TABLE II. The table shows, for each power and field configuration: (1) the peak field strength $E_0/E_{\rm cr}$; and (2) the maximum attainable $\chi_0=\gamma_0 E_0/E_{\rm cr}$ for a 10 GeV electron interacting with the peak field. Values where $\alpha\chi_0^{2/3}>1$ are presented in bold.

4π-focused optical field; (3) an $f/1$-focused XUV field; and (4) a dipole focused XUV field using $6\times f/1$ as described in Section II C. We have here assumed an optical wavelength of 0.8 µm and that the plasma conversion is performed at $10^{22}\,\mathrm{W/cm^2}$ for the XUV fields. We also present the maximum attainable χ, for a 10 GeV electron interacting with the peak field. For a plasma conversion at $10^{23}\,\mathrm{W/cm^2}$ the peak fields, as well as the maximum χ, will be increased by a factor of $13/\sqrt{10}\approx4.1$. Because the minimum power required to reach an intensity of $10^{22}\,\mathrm{W/cm^2}$ ($10^{23}\,\mathrm{W/cm^2}$) at the plasma converter is $\mathcal{P}^{\rm min}=0.087\,\mathrm{PW}$ (0.87 PW), assuming $f/1$ focusing, we restrict ourselves to laser powers above 1 PW.

In Table III we present an estimate for the Schwinger pair production by applying equation B1 to both an optical dipole wave and to a dipole focused XUV field, as described by equation 7. The estimates are presented as the number of pairs per optical cycle, disregarding any potential secondary effects due to the produced pairs. To evaluate if pair plasma effects may nevertheless come into play, we further estimate the density of the produced pairs and compare it to the plasma critical density $n_{\rm cr}=\sqrt{1+a_0^2}n_{\rm c}$. We obtain the density estimate by assuming that all pairs produced will be distributed within a volume $\mathcal{V}$, taken as the volume where the field strength is $E/E_0>1/2$. For the optical dipole, the plasma critical density is $n_{\rm c}=1.7\times10^{21}\,\mathrm{cm^{-3}}$ and the characteristic field volume is $\mathcal{V}=4.9\times10^{-14}\,\mathrm{cm^3}$. For the dipole focused XUV field, the plasma critical density is $n_{\rm c}=1.1\times10^{27}\,\mathrm{cm^{-3}}$ and the characteristic field volume is $\mathcal{V}=5.2\times10^{-22}\,\mathrm{cm^3}$, where plasma conversion at $10^{22}\,\mathrm{W/cm^2}$ has been assumed and where the wavelength has been taken as the characteristic size of the field ($2R$) as defined in equation 7.

Finally, we also present estimates for the multiplication factor due to Breit-Wheeler pair production, over a single optical cycle. For the optical dipole the growth rate is given by $\Gamma(\mathcal{P})\approx3.21T^{-1}(\mathcal{P}^{1/3}-\mathcal{P}_{\rm min}^{1/3})$, where $\mathcal{P}_{\rm min}=7.2\,\mathrm{PW}$ and T is the optical period [14]. For the dipole-focused XUV field we instead estimate an upper bound for the multiplication factor. This is done by computing the growth factor due to Breit-Wheeler pair production for a seed particle in a constant field of strength $E_0/E_{\rm cr}$ (even though we are aware that a tree-level calculation of the Breit-Wheeler rate will not be valid for very high χ), and assuming that all generated particles are produced with the same constant $\chi_0=\gamma_0E_0/E_{\rm cr}$ as the parent particle. The growth factor is taken as the number of particles after a time R/c, corresponding to the typical time it would take a seed particle to escape the field.

Table III shows that the number of pairs produced through the Schwinger mechanism is greatly increased for the dipole-focused XUV field, due to the increased field strength. At the same time, the cascade growth rate (due to Compton scattering and Breit-Wheeler pair production) is likely reduced over a single cycle. Over multiple cycles, the XUV field is even less likely to maintain a cascade, as the field now constitutes individual burst with no means of continuous particle trapping between cycles. The table further suggests that the number of Schwinger pairs produced

	$\mathcal{P}$, PW	$E_0/E_{\rm cr}$	$N_p^{\rm Schwinger}$	$N_p^{\rm Schwinger}/\mathcal{V}n_{\rm cr}$	ΓT
Optical	1	2.3×10^{-3}	-	-	-
	10	7.4×10^{-3}	2.1×10^{-169}	1.0×10^{-180}	0.72
	100	2.3×10^{-2}	4.1×10^{-43}	6.1×10^{-55}	8.7
	1000	7.4×10^{-2}	7.4×10^{-2}	3.5×10^{-14}	25.9
XUV	1	2.2	3.9×10^{10}	7.3×10^{1}	$\ll1.5$
	10	7.1	7.8×10^{12}	4.6×10^{3}	$\ll2.9$
	100	22	5.5×10^{14}	1.0×10^{5}	$\ll6.3$
	1000	71	2.5×10^{16}	1.5×10^{6}	$\ll18$

TABLE III. The table shows, for different values of $\mathcal{P}$ and for two different field configurations: (1) the peak field strength $E_0/E_{\rm cr}$; (2) the estimated number of pairs produced per optical cycle through the Schwinger mechanism $N_p^{\rm Schwinger}$; (3) the estimated pair plasma density normalized to the critical density $N_p^{\rm Schwinger}/\mathcal{V}n_{\rm cr}$; and (4) the particle growth rate due to Breit-Wheeler pair creation ΓT. These results represent an upper limit on the pair creation yield, assuming the field is an electric dipole wave.

would surpass the plasma critical density, if entirely contained within the strong-field region, which might hinder the field strength from reaching its theoretical maximum. Whether a field strength greater than $E_{\rm cr}$ would always, if at all, generate such a dense pair plasma through the Schwinger mechanism, would require more detailed analysis accounting for the particle dynamics, which lies outside the scope of this paper.